

Open Research Online

The Open University's repository of research publications
and other research outputs

Fluorine effect on As diffusion in Ge

Journal Item

How to cite:

Impellizzeri, G.; Boninelli, S.; Priolo, F.; Napolitani, E.; Spinella, C.; Chroneos, A. and Bracht, H. (2011). Fluorine effect on As diffusion in Ge. *Journal of Applied Physics*, 109(11), article no. 113527.

For guidance on citations see [FAQs](#).

© 2011 American Institute of Physics

Version: Version of Record

Link(s) to article on publisher's website:
<http://dx.doi.org/doi:10.1063/1.3592962>

Copyright and Moral Rights for the articles on this site are retained by the individual authors and/or other copyright owners. For more information on Open Research Online's data [policy](#) on reuse of materials please consult the policies page.

oro.open.ac.uk

Fluorine effect on As diffusion in Ge

G. Impellizzeri,^{1,a)} S. Boninelli,¹ F. Priolo,¹ E. Napolitani,² C. Spinella,³ A. Chroneos,⁴ and H. Bracht⁵

¹*MATIS IMM-CNR and Dipartimento di Fisica e Astronomia, Università di Catania, Via S. Sofia 64, 95123 Catania, Italy*

²*MATIS IMM-CNR and Dipartimento di Fisica, Università di Padova, Via Marzolo 8, 35131 Padova, Italy*

³*IMM-CNR, VIII Strada 5, 95121 Catania, Italy*

⁴*Department of Materials Science and Metallurgy, University of Cambridge, Cambridge CB2 3QZ, United Kingdom*

⁵*Institute of Materials Physics, University of Münster, Wilhelm-Klemm-Str. 10, 48149 Münster, Germany*

(Received 9 March 2011; accepted 22 April 2011; published online 8 June 2011)

The enhanced diffusion of donor atoms, via a vacancy (*V*)-mechanism, severely affects the realization of ultrahigh doped regions in miniaturized germanium (Ge) based devices. In this work, we report a study about the effect of fluorine (F) on the diffusion of arsenic (As) in Ge and give insights on the physical mechanisms involved. With these aims we employed experiments in Ge co-implanted with F and As and density functional theory calculations. We demonstrate that the implantation of F enriches the Ge matrix in *V*, causing an enhanced diffusion of As within the layer amorphized by F and As implantation and subsequently regrown by solid phase epitaxy. Next to the end-of-range damaged region F forms complexes with Ge interstitials, that act as sinks for *V* and induce an abrupt suppression of As diffusion. The interaction of Ge interstitials with fluorine interstitials is confirmed by theoretical calculations. Finally, we prove that a possible F-As chemical interaction does not play any significant role on dopant diffusion. These results can be applied to realize abrupt ultra-shallow *n*-type doped regions in future generation of Ge-based devices. © 2011 American Institute of Physics. [doi:10.1063/1.3592962]

I. INTRODUCTION

Germanium has been the first semiconductor in the microelectronic industry but it was replaced by silicon in the sixties and since then it was almost abandoned. Recently, Ge has received renewed scientific and industrial interest¹ due to its strong potential as high-mobility carrier material^{2,3} together with its high compatibility with the existing Si-based technology.

Implantation and diffusion of dopants are crucial steps for the realization of Ge-based devices. Although *p*-type dopants, such as B,^{4,5} Al,⁶ Ga,^{7,8} and In (Refs. 9 and 10) exhibit a low diffusivity in Ge, *n*-type dopants, such as P,^{4,11} As,^{4,12} and Sb (Ref. 4) have a high diffusivity, hampering the formation of ultra-shallow junctions in Ge. It is today well assessed that both intrinsic and extrinsic diffusion of donor dopants in Ge is fully described on the basis of a vacancy (*V*)-mediated mechanism.^{13,14}

In the past, co-doping with C was considered in order to reduce the enhanced donor diffusion in Ge.^{15,16} It was found that co-doping with C leads to a retardation of donor atom transport via the formation of less mobile carbon-vacancy-donor clusters.^{15,16} A recent theoretical study by some of the present authors calculated that F might suppress donor diffusion in Ge under equilibrium conditions by affecting the concentration of free *V*.¹⁷ Presently, however, there is no experimental evidence of the role of F in the microscopic diffusion mechanism of donor dopants in Ge. The effect of F in engineering point defects (vacancies and self-interstitials)

and, as a consequence, in affecting the diffusion of dopants in Si was extensively investigated by our group, and consists in the annihilation of self-interstitials at nano-bubbles introduced in the crystalline matrix through a complex mechanism of F segregation and incorporation within the crystalline phase.^{18–26}

The aim of this work is to study in detail the effect of F in modifying As diffusion in Ge. For this purpose, we performed structural and chemical characterizations of Ge samples co-implanted with F and As and annealed with different thermal budgets. We also performed atomistic calculations on the stability of defect complexes formed between F and point defects. Crossing the experimental and theoretical results we clarify the physical mechanisms by which F modifies the point defect density and, as a consequence, the diffusion of As in Ge. Our results shed light on the behavior of F in Ge and might allow a higher control of As and, in general, of *n*-type dopant diffusion for the fabrication of advanced high-performance Ge-based devices.

II. METHODS

A. Experimental

A germanium Czochralski wafer, (100)-oriented, *p*-type (with a bulk resistivity higher than 40 Ω·cm) was implanted with F⁺ and then with As⁺ ions at fluences (energies) of 1×10^{15} F/cm² (35 keV) and 3×10^{13} As/cm² (50 keV). The arsenic implantation was designed to fall entirely within the F-enriched region.²⁷ As will be illustrated in Sec. III A, such an implantation induced an amorphization of the Ge matrix

^{a)}Electronic mail: giuliana.impellizzeri@ct.infn.it.

down to a depth of ~ 80 nm. A wafer preamorphized with Ge^+ ions at fluence (energy) of 2×10^{14} Ge/cm^2 (100 keV) and then implanted with As^+ ions was used as reference sample. The energy and fluence of the Ge^+ ions implantation were chosen to amorphize the Ge matrix to about the same depth of the sample implanted with F and As.²⁸ After implantation a 40 nm- SiO_2 cap was deposited by sputtering at room temperature onto all investigated samples. The silicon dioxide cap was used to avoid any possible dopant out-diffusion during the following thermal treatments.²⁹ The samples were annealed for 1 h at the temperatures of 400, 450, 500, or 600 °C. All thermal treatments were performed in a conventional furnace under a controlled N_2 flux.

Rutherford backscattering spectrometry (RBS) analyses in channeling configuration were carried out to investigate the thickness of the amorphous layers formed by ion implantation. Transmission electron microscopy (TEM) was performed with a 200 keV 2010 JEOL instrument to investigate the implantation-induced damage and the residual crystalline disorder after the thermal treatments. Cross-section TEM (X-TEM) samples were prepared, after a dip in HF to remove the silicon dioxide, by means of standard X-TEM preparation with mechanical grinding and ion milling performed in a GATAN-PIPS apparatus at low energy (3 keV Ar) and low incidence (7°) to minimize the irradiation damage.

Chemical depth profiles of F and As were obtained by secondary ion mass spectrometry (SIMS) using a Cameca IMS-4f instrument with a Cs^+ 14.5 keV sputtering beam and collecting $^{19}\text{F}^{76}\text{Ge}^-$ and $^{75}\text{As}^{76}\text{Ge}^-$ molecular ions. The analyses were performed without removing the silicon dioxide layer. The depth scale of the profiles was calibrated by measuring the crater depths with a profilometer and assuming constant erosion rates. Dedicated measurements revealed almost equal erosion rates for the silicon dioxide layer and the germanium bulk.

B. Theoretical

In order to investigate the interactions between F and self-interstitials in Ge, we employed the density functional theory (DFT) code CASTEP³⁰ using the Perdew-Burke-Ernzerhof generalized gradient approximation functional³¹ and ultrasoft pseudopotentials.³² A supercell of 64 site tetragonal diamond structure Ge was repeated in space using periodic boundary conditions. The plane wave basis energy cutoff was 350 eV. $2 \times 2 \times 2$ Monkhorst-Pack (MP)³³ k-point sampling was used. The unit-cell parameters and the atomic coordinates were relaxed using energy minimization until the largest forces were less than 0.05 eV/Å with a total energy convergence tolerance not exceeding 10^{-5} eV/atom. This methodology adequately describes the defect chemistry of Ge and related materials as was demonstrated by comparing the predictions with experimental results.^{34,35}

The computational parameters and supercell size in the present study sufficiently describe the system as discussed in recent works of related systems in Ge and other group-IV semiconductors.^{36–38} This is because in the 64 supercell the fluorine atoms and other defects are adequately separated from their periodic images. At these distances the defect-

defect interactions are very small and therefore the dopant and its periodic image interactions will not affect the results. As demonstrated by Probert and Payne³⁶ larger MP k-point grids and supercell sizes lead to small differences in the defect energies. In Ge typical energy differences are less than 0.05 eV, whereas the trends are maintained.

The attraction between point defect [Ge vacancies (V) or Ge interstitials (Ge_i)], As substitutional atoms, and F interstitials can be quantified by calculating the binding energies. The binding energy of n F interstitial atoms to m V and x As atoms to form an $\text{As}_x\text{V}_m\text{F}_n$ cluster in Ge is given by

$$E_b(\text{As}_x\text{V}_m\text{F}_n\text{Ge}_{N-x-m}) = E(\text{As}_x\text{V}_m\text{F}_n\text{Ge}_{N-x-m}) - xE(\text{AsGe}_{N-1}) - nE(\text{FGe}_N) - mE(\text{VGe}_{N-1}) + (x+m+n-1)E(\text{Ge}_N), \quad (1)$$

where $E(\text{As}_x\text{V}_m\text{F}_n\text{Ge}_{N-x-m})$ is the energy of a N lattice supercell that contains $N-x-m$ Ge atoms, n F atoms, m V and x As atoms; $E(\text{AsGe}_{N-1})$ is the energy of a supercell that contains one As and $N-1$ Ge atoms; $E(\text{FGe}_N)$ is the energy of a supercell that contains one F interstitial and N Ge atoms; $E(\text{VGe}_{N-1})$ is the energy of a supercell that contains one V and $N-1$ Ge atoms; and $E(\text{Ge}_N)$ is the energy of a supercell that contains N Ge atoms.

Similarly the binding energy to form a FGe_i pair is given by

$$E_b(\text{FGe}_i\text{Ge}_N) = E(\text{FGe}_i\text{Ge}_N) - E(\text{FGe}_N) - E(\text{Ge}_i\text{Ge}_N) + E(\text{Ge}_N), \quad (2)$$

where $E(\text{FGe}_i\text{Ge}_N)$ is the energy of a N lattice supercell that contains N Ge atoms (at their diamond lattice sites), a Ge interstitial and a F interstitial; $E(\text{Ge}_i\text{Ge}_N)$ is the energy of a N lattice supercell that contains N Ge atoms (at their diamond lattice sites) and a Ge interstitial. According to these equations a negative binding energy indicates that the cluster is more energetically favorable with respect to its constituent components.

III. RESULTS

A. Experiment

Figures 1(a) and 1(b) show the concentration profiles of F (lines with circles) and As (lines without circles) measured by SIMS, in samples implanted with 1×10^{15} F/cm^2 at 35 keV and then with 3×10^{13} As/cm^2 at 50 keV and annealed up to 600 °C, while Fig. 1(c) shows the concentration profile of As (lines) in the reference samples without F. The SiO_2/Ge interface (at a depth of ~ 40 nm) is indicated by a vertical straight line. The rise of the F and As signals at the SiO_2/Ge interface (i.e., the peaks at the depth of ~ 40 nm, as well as the tails extending down to ~ 80 nm) is an artifact of the SIMS technique due to mass interferences, interface transient effects, and atom relocation during the analyses. Annealing at 400 °C for 1 h seems not to affect the As profile significantly, both in the sample with F and in the reference sample [dashed-dotted lines in Figs. 1(b) and 1(c)], whereas the F profile changes considerably [dashed-dotted line with circles

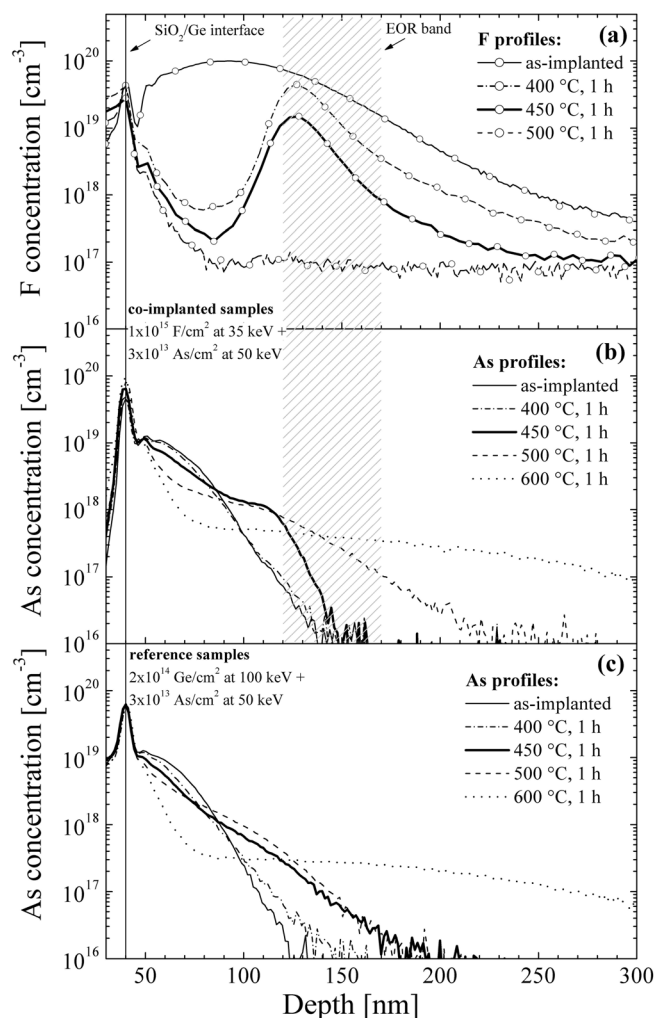


FIG. 1. Concentration profiles of F (lines with circles) and As (lines without circles) in the samples co-implanted with F, (a) and (b), respectively, and As (lines) in the reference samples without F (c), just after the implantations (straight lines) and after annealing for 1 h at 400 °C (dashed-dotted lines), 450 °C (straight thick lines), 500 °C (dashed lines), or 600 °C (dotted lines). The vertical rectangle indicates the region containing the band of EOR defects, which are present in the sample enriched with F up to the temperatures of 450 °C.

in Fig. 1(a)]. In fact, about 80% of the implanted F fluence is lost during the thermal treatment. A pronounced dip of the F profile at ~ 80 nm (40 nm below the SiO₂/Ge interface) and a pileup (with a concentration peak of 4.5×10^{19} F/cm³) at a depth of ~ 125 nm (~ 85 below the SiO₂/Ge interface) are formed. Such a pileup is still present after 1 h at 450 °C (thick straight line with circles), but with a lower peak concentration of 1.5×10^{19} F/cm³ with respect to the one obtained after 400 °C.

This F behavior is striking and has a significant and interesting influence on the diffusion of As. In fact, the As profile, obtained after 1 h at 450 °C [thick straight line in Fig. 1(b)], shows a significant diffusion in the region between the SiO₂/Ge interface and the depth of ~ 110 nm (i.e., ~ 70 nm below the SiO₂/Ge interface), but an abrupt interruption of the diffusion is present next to the accumulation peak of fluorine. By comparing the above results with the behavior of the reference sample without F [thick straight line in Fig. 1(c)], it is clear that the F influences the As behavior with two different

mechanisms: (a) an enhancement of the diffusion within the re-grown layer down to a depth of ~ 110 nm (i.e., ~ 70 nm below the SiO₂/Ge interface), and (b) a suppression of the As diffusion just before the F accumulation peak. The enhancement of the diffusion can be evidenced considering the As concentration at the depth of 110 nm in the reference sample without F: 4.5×10^{17} As/cm³, with that in the F-implanted sample: 1.1×10^{18} As/cm³ (higher in this last sample by a factor of 2.4). The suppression of As diffusion next to the accumulation peak of F is remarkable as it might limit the diffusion of As in Ge for ultra-shallow junction formation technology. Interestingly, the resulting profile at 450 °C in Fig. 1(b) is much steeper than the as-implanted profile.

By increasing the annealing temperature at 500 °C a complete loss of F is observed, the F profile falls below the measurement background of 8×10^{16} F/cm³ [dashed line with circles in Fig. 1(a)]. Concerning the As profiles, after 1 h at 500 °C the As [dashed line in Fig. 1(b)] shows an enhanced diffusion in the sample enriched with F with respect to the reference sample [dashed line in Fig. 1(c)] and this nicely correlates with the complete loss of F observed in Fig. 1(a) confirming that the suppression of As diffusion at the depth of ~ 120 nm observed at 450 °C is related to F. After 600 °C the diffusion profiles of As are similar in samples with and without F [dotted lines in Figs. 1(b) and 1(c)]. This demonstrates that the effect of fluorine on As diffusion vanishes at high temperatures.

It is worth to note that the chemical profiles of F after the different thermal treatments seem to not be affected by the presence of As nor any accumulation of F in correspondence with As is observed [see Fig. 1(a)]. These results likely suggest that there is not a direct interaction between F and As atoms in form of FAs complexes.

More insights on the above phenomena can be obtained from the X-TEM images reported in Fig. 2. Panel (a) shows

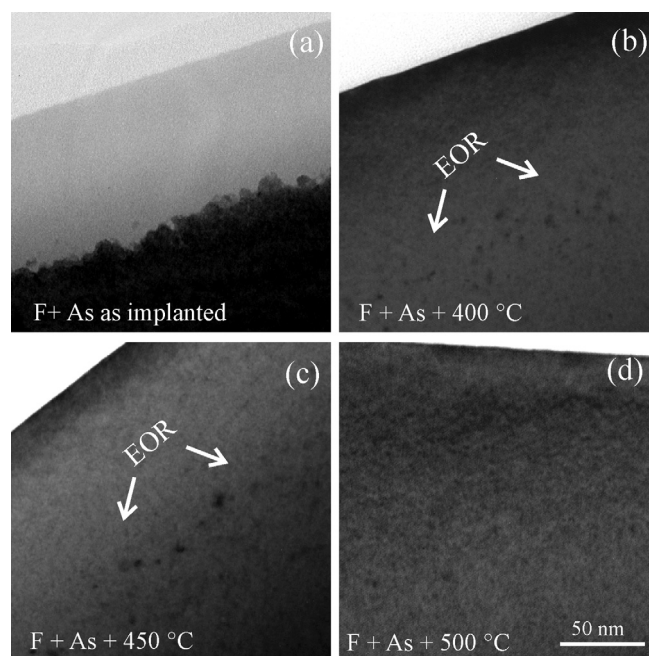


FIG. 2. TEM cross section views of the samples co-implanted with F and As just after the implantations (a) and after annealing for 1 h at 400 °C (b), 450 °C (c), or 500 °C (d).

that the sample co-implanted with F and As presents, just after the implantation, an amorphous layer extending from the surface down to a depth of ~ 80 nm (note that the oxide layer was removed before the analyses). After 1 h at 400 °C [Fig. 2(b)] the amorphous layer is completely re-grown by solid phase epitaxy (SPE) with the re-crystallized region free of detectable defects, but an end-of-range (EOR) defect band, ~ 50 nm thick, is observed beyond the original amorphous/crystalline interface, i.e., at ~ 80 –130 nm below the Ge surface. After 1 h at 450 °C, these defects survive in the F-enriched sample, as shown in Fig. 2(c). The defect band is also schematically represented in Figs. 1(a) and 1(b) by a vertical rectangle. These EOR defects have the form of small dots and are similar to those observed by the group of A. Claverie after SPE regrowth of amorphous layers created by ion implantation in Ge.³⁹ They identified these defects as interstitial-type, as confirmed by Bisognin *et al.* with high resolution x-ray diffraction measurements.⁴⁰ The reference sample (not shown) presents after ion implantation an amorphous layer similar to that reported in Fig. 2(a) (as verified by RBS analysis) but, in contrast to the sample enriched with F, after annealing at 400 °C for 1 h no defects are observed by X-TEM within the sensitivity of the technique. This is in agreement with the results recently published by our group showing that EOR defects formed by Ge^+ ion implantation, i.e., without any effect of impurities included intentionally, should disappear, according to X-TEM images, after 1 h annealing at a temperature above a threshold located between 380 °C and 420 °C.⁴¹ Therefore, F implantation affects not only As diffusion but also increases significantly the stability of the EOR defects. In addition, it is important to note that the band of EOR defects shown in Figs. 2(b) and 2(c) has the same depth as the F pileup shown in Fig. 1(a). These observations strongly support the idea that the additional thermal budget needed to dissolve the EOR defects in the sample enriched by F is due to a decoration of the defects by F atoms that significantly increase their stability. The above considerations led us to assume the formation of FGe_i clusters, whose existence is supported by the theoretical investigation reported in Sec. III B, and suggest that such FGe_i clusters are the cause of the interesting diffusive behavior of As shown in Fig. 1(b). By increasing the temperature to 500 °C, the EOR defects are completely dissolved also in the sample enriched with F, as shown in the X-TEM image of Fig. 2(d). This nicely correlates with the complete loss of F shown in Fig. 1(a) and further supports the idea of a stabilization of EOR defects due to their decoration with F atoms.

B. Theory

In Ge fluorine interstitial can occupy the bond-center position or the tetrahedral position¹⁷ [see Lopez *et al.* for a detailed discussion of F interstitials in Si (Ref. 20)]. We recently found the bond-center position for the F interstitial to be favored by 0.38 eV compared to the tetrahedral position.¹⁷ These predictions are consistent with previous results for F interstitial in Si.^{20,42}

In previous DFT work we calculated that F_nV_m clusters can form in F-enriched Ge where there is a high concentra-

TABLE I. Binding energies E_b (eV) for clusters formed between V, Ge_i , As substitutional atoms, and F interstitials in Ge.

Defect cluster	E_b (eV)
FV	-1.19 ^a
F_2V	-2.22 ^a
F_3V	-3.27 ^a
F_4V	-5.00 ^a
AsV	-0.60 ^b
AsVF	-1.76 ^a
AsVF ₂	-2.87 ^a
AsVF ₃	-4.00 ^a
FGe_i	-0.60

^aReference 17.

^bReference 44.

tion of F and a supersaturation of vacancies.¹⁷ The driving force for the formation of F_nV_m clusters is the saturation by F of the dangling bonds created by the lattice vacancies. F_nV_m clusters for which all the dangling bonds are saturated (i.e., F_4V or F_6V_2) exhibit the highest binding energies (refer to Eq. (1) and Table I for the binding energies of F_nV clusters). This is analogous to previous findings in Si.⁴² We demonstrated recently, using a mass action approach, that the most bound clusters are not necessarily the most populous.¹⁷ Indeed smaller clusters such as FV, F_2V_2 , or F_3V_2 can often dominate the concentration of F_nV_m related clusters especially at high temperatures (above 850 K).¹⁷

Previously it was assumed that the F_nV_m clusters are the dominant defects in Ge enriched with F.¹⁷ It is determined, however, that Ge_i can also become dominant next to the EOR damaged region. Here we calculated the attraction between a F interstitial atom and a Ge interstitial atom by calculating the binding energy of a FGe_i pair [refer to Eq. (2)]. In the present study, we predict that the FGe_i pair, consisting of a F interstitial at bond-center position and a Ge_i at tetrahedral position, is bound by -0.60 eV. Although the binding energy of the FGe_i pair is smaller compared to the binding energies of the F_nV_m clusters reported in Table I it can become important when there is a supersaturation of Ge_i (i.e., next to the EOR region). This is because a supersaturation of Ge_i will lead to the suppression of vacancies. Assuming a simple mass action treatment (as the one in Ref. 17) the suppression of vacancies will effectively lead to the demise of the F_nV_m and related clusters such as AsVF_n (Table I). This can lead to the domination of the FGe_i pairs and related clusters even though their binding energies are relatively small (Table I). Therefore, in the event of an encounter between a F interstitial and a Ge_i it is likely to form a FGe_i pair that will impact the diffusion properties.

IV. DISCUSSION

Based on the experimental and theoretical results, the peculiar diffusion behavior of As in presence of F [see Fig. 1(b)] can be described through the following scenario. During SPE at 400 °C most of F leaves the sample [see Fig. 1(a)]. After 450 °C an excess of V located within the region between the SiO_2/Ge interface and the defect band, probably

left by the SPE process in presence of F, could be responsible for the observed enhanced diffusion of As [see Fig. 1(b) and for comparison Fig. 1(c)]. In addition, next to the F accumulation peak the possible formation of FGe_i complexes represents a sink for V that is considered to suppress the diffusion of As [see Figs. 1(a) and 1(b)]. The formation of FGe_i complexes is supported by several observations, such as the superposition of the EOR defect band with the F pileup, the correlation of the dissolution of the EOR defects with the erosion of the F pileup and the stabilization of the EOR defects in the presence of F. The existence of FGe_i clusters is also confirmed by theoretical calculations (see Sec. III B). Therefore, these two different regions, one rich in vacancies and one rich in interstitials, might explain the opposite diffusive behavior of As observed within the re-grown layer (diffusion enhanced) and close to the EOR defects (diffusion suppressed). The latter effect is crucial, as it demonstrates the ability of F in blocking the diffusion of the dopants via a V -mediated mechanism.

After annealing at 500 °C, a complete loss of F is observed [see Fig. 1(a)]. This result goes along with the complete dissolution of the EOR defects observed by X-TEM [see Fig. 2(d)]. Probably at this temperature, the FGe_i clusters completely dissolve leaving as a consequence the F free to diffuse apparently for long distances. The observed high-mobility of F in Ge when not trapped by a defect is striking and demands further investigations. Concerning the As profiles, after 500 °C the As shows an enhanced diffusion in the sample enriched with F with respect to the reference sample without F [see Figs. 1(b) and 1(c)]. The reason for this enhanced diffusion is compatible with the complete dissolution of the EOR defects (i.e., traps for V). The dissolution of EOR defects leaves the As free to migrate and a material free of sinks for V . A residual concentration of V may still be present at this temperature within the re-grown layer that causes the enhanced As diffusion. After 600 °C the diffusion profiles of As are similar in samples with and without F [see Figs. 1(b) and 1(c)]. This demonstrates that the effect of fluorine on As diffusion and defect evolution vanishes at high temperatures.

In addition, we have excluded a hypothetical chemical bond between F and As atoms. This result is also confirmed by DFT calculations in conjunction with mass action analysis, which calculated that the concentration of clusters containing both donor atoms and F atoms are never of importance.¹⁷

Our study shows that F behaves in a similar way in Ge and in Si. In details, the observed long-range migration of F [see Fig. 1(a)], the ability of F to enrich the Ge matrix in V [responsible for the observed enhanced diffusion of As, see Figs. 1(b) and 1(c)] and the decoration of the EOR defects by F atoms [see Fig. 1(a)] are three physical phenomena yet showed in Si.^{18–26,43}

V. CONCLUSIONS

In conclusion, we presented a detailed study concerning the effect of F in modifying the diffusion of As in Ge. For this purpose, we performed structural and chemical charac-

terizations of Ge samples co-implanted with F and As and annealed with different thermal budgets. We propose that the implantation of F enriches the Ge matrix in V . This enhances the diffusion of As within the layer amorphized by F and As implantation, that is subsequently re-grown by SPE. Next to the EOR damaged region F forms complexes with Ge interstitials, which represent efficient sinks for V and induce a suppression of As diffusion. This result is crucial, as it demonstrates the ability of F in blocking dopant diffusion mediated by V . The formation of FGe_i complexes is supported by atomistic calculations. Moreover, we conclude that the F-As chemical interaction does not play any significant role in dopant diffusion, in good agreement with theoretical results. Our results, showing the ability of F in modifying the point defects density of the Ge matrix, shed light on the F behavior in Ge and allow a better control of n -type dopant diffusion during Ge-based device processing.

ACKNOWLEDGMENTS

The authors wish to thank G. Scapellato (MATIS IMM-CNR and University of Catania) for RBS analyses, Dr. M. P. Miritello (MATIS IMM-CNR) for sputtering depositions, C. Percolla (MATIS IMM-CNR), S. Tati (MATIS IMM-CNR), and R. Storti (University of Padova) for their expert technical assistance. A. C. is a Visiting Academic at Imperial College London and acknowledges computing resources provided by the HPC facility.

- ¹C. Claeys and E. Simoen, *Germanium-Based Technologies - From Materials to Devices* (Elsevier, Amsterdam, 2007).
- ²S. M. Sze and J. C. Irvin, *Solid State Electron.* **11**, 599 (1968).
- ³S. Mirabella, G. Impellizzeri, A. M. Piro, E. Bruno, and M. G. Grimaldi, *Appl. Phys. Lett.* **92**, 251909 (2008).
- ⁴C. O. Chui, K. Gopalakrishnan, P. B. Griffin, J. D. Plummer, and K. C. Saraswat, *Appl. Phys. Lett.* **83**, 3275 (2003).
- ⁵S. Uppal, A. F. W. Willoughby, J. M. Bonar, N. E. B. Cowern, T. Grasby, R. J. H. Morris, and M. G. Dowsett, *J. Appl. Phys.* **96**, 1376 (2004).
- ⁶P. Dörner, W. Gust, A. Lodding, H. Odelius, B. Predel, and U. Roll, *Acta Metall.* **30**, 941 (1982).
- ⁷U. Södervall, H. Odelius, A. Lodding, U. Roll, B. Predel, W. Gust, and P. Dörner, *Phil. Mag. A* **54**, 539 (1986).
- ⁸G. Impellizzeri, S. Mirabella, A. Irrera, M. G. Grimaldi, and E. Napolitani, *J. Appl. Phys.* **106**, 013518 (2009).
- ⁹P. Dörner, W. Gust, A. Lodding, H. Odelius, B. Predel, and U. Roll, *Z. Metallkd.* **73**, 325 (1982).
- ¹⁰R. Kube, H. Bracht, A. Chroneos, M. Posselt, and B. Schmidt, *J. Appl. Phys.* **106**, 063534 (2009).
- ¹¹A. Satta, E. Simoen, R. Duffey, T. Janssens, T. Clarysse, A. Benedetti, M. Meuris, and W. Vandervorst, *Appl. Phys. Lett.* **88**, 162118 (2006).
- ¹²E. Vainonen-Ahlgren, T. Ahlgren, J. Likonen, S. Lehto, J. Keinonen, W. Li, and J. Haapamäki, *Appl. Phys. Lett.* **77**, 690 (2000).
- ¹³S. Brotzmann and H. Bracht, *J. Appl. Phys.* **103**, 033508 (2008).
- ¹⁴A. Chroneos, H. Bracht, R. W. Grimes, and B. P. Uberuaga, *Appl. Phys. Lett.* **92**, 17103 (2008).
- ¹⁵S. Brotzmann, H. Bracht, J. L. Hansen, A. N. Larsen, E. Simoen, E. E. Haller, J. S. Christensen, and P. Werner, *Phys. Rev. B* **77**, 235207 (2008).
- ¹⁶A. Chroneos, R. W. Grimes, B. P. Uberuaga, and H. Bracht, *Phys. Rev. B* **77**, 235208 (2008).
- ¹⁷A. Chroneos, R. W. Grimes, and H. Bracht, *J. Appl. Phys.* **106**, 063707 (2009).
- ¹⁸G. Impellizzeri, J. H. R. dos Santos, S. Mirabella, F. Priolo, E. Napolitani, and A. Camera, *Appl. Phys. Lett.* **84**, 1862 (2004).
- ¹⁹S. Mirabella, G. Impellizzeri, E. Bruno, L. Romano, M. G. Grimaldi, F. Priolo, E. Napolitani, and A. Camera, *Appl. Phys. Lett.* **86**, 121905 (2005).
- ²⁰G. M. Lopez, V. Fiorentini, G. Impellizzeri, S. Mirabella, and E. Napolitani, *Phys. Rev. B* **72**, 45219 (2005).

- ²¹G. Impellizzeri, S. Mirabella, F. Priolo, E. Napolitani, and A. Carnera, *J. Appl. Phys.* **99**, 103510 (2006).
- ²²S. Boninelli, A. Claverie, G. Impellizzeri, S. Mirabella, F. Priolo, E. Napolitani, and F. Cristiano, *Appl. Phys. Lett.* **89**, 171916 (2006).
- ²³G. Impellizzeri, S. Mirabella, A. M. Piro, M. G. Grimaldi, F. Priolo, F. Giannazzo, V. Raineri, E. Napolitani, and A. Carnera, *Appl. Phys. Lett.* **91**, 132101 (2007).
- ²⁴S. Boninelli, G. Impellizzeri, S. Mirabella, F. Priolo, E. Napolitani, N. Cherkashin, and F. Cristiano, *Appl. Phys. Lett.* **93**, 061906 (2008).
- ²⁵D. De Salvador, G. Bisognin, E. Napolitani, M. Mastromatteo, N. Baggio, A. Carnera, F. Boscherini, G. Impellizzeri, S. Mirabella, S. Boninelli, F. Priolo, and F. Cristiano, *Appl. Phys. Lett.* **95**, 101908 (2009).
- ²⁶M. Mastromatteo, D. De Salvador, E. Napolitani, F. Panciera, G. Bisognin, A. Carnera, G. Impellizzeri, S. Mirabella, and F. Priolo, *Phys. Rev. B* **82**, 155323 (2010).
- ²⁷J. F. Ziegler, J. P. Biersack, and U. Littmark, *The Stopping and Range of Ions in Solids*, Vol. 1 of series Stopping and Ranges of Ions in Matter (Pergamon Press, New York, 1984), <http://www.srim.org>.
- ²⁸G. Impellizzeri, S. Mirabella, and M. G. Grimaldi, *Appl. Phys. A* **103**, 323 (2011).
- ²⁹C. Jasper, L. Rubin, C. Lindfors, K. S. Jones, and J. Oh, *Proceedings of the Ion Implantation Techniques* (The IEEE, New York, 2002), p. 548.
- ³⁰M. D. Segall, P. J. D. Lindan, M. J. Probert, C. J. Pickard, P. J. Hasnip, S. J. Clark, and M. C. Payne, *J. Phys.: Condens. Matter* **14**, 2717 (2002).
- ³¹J. Perdew, K. Burke, and M. Ernzerhof, *Phys. Rev. Lett.* **77**, 3865 (1996).
- ³²D. Vanderbilt, *Phys. Rev. B* **41**, 7892 (1990).
- ³³H. J. Monkhorst and J. D. Pack, *Phys. Rev. B* **13**, 5188 (1976).
- ³⁴D. Caliste, P. Pochet, T. Deutsch, and F. Lançon, *Phys. Rev. B* **75**, 125203 (2007).
- ³⁵A. Chroneos, H. Bracht, C. Jiang, B. P. Uberuaga, and R. W. Grimes, *Phys. Rev. B* **78**, 195201 (2008).
- ³⁶M. I. J. Probert and M. C. Payne, *Phys. Rev. B* **67**, 075204 (2003).
- ³⁷A. Chroneos and C. A. Londos, *J. Appl. Phys.* **107**, 093518 (2010).
- ³⁸J. Coutinho, R. Jones, P. R. Briddon, and S. Öberg, *Phys. Rev. B* **62**, 10824 (2000).
- ³⁹S. Koffel, N. Cherkashin, F. Houdellier, M. J. Hytch, G. Benassayag, P. Scheiblin, and A. Claverie, *J. Appl. Phys.* **105**, 126110 (2009).
- ⁴⁰G. Bisognin, S. Vangelista, and E. Bruno, *Mater. Sci. Eng. B* **154–155**, 64 (2008).
- ⁴¹E. Napolitani, G. Bisognin, E. Bruno, M. Mastromatteo, G. Scapellato, S. Boninelli, D. De Salvador, S. Mirabella, C. Spinella, A. Carnera, and F. Priolo, *Appl. Phys. Lett.* **96**, 201906 (2010).
- ⁴²M. Diebel and S. T. Dunham, *Phys. Rev. Lett.* **93**, 245901 (2004).
- ⁴³P. Lopez, L. Pelaz, R. Duffy, P. Meunier-Beillard, F. Roozeboom, K. van der Tak, P. Breimer, J. G. M. van Berkum, M. A. Verheijen, and M. Kaiser, *J. Appl. Phys.* **103**, 093538 (2008).
- ⁴⁴A. Chroneos, B. P. Uberuaga, and R. W. Grimes, *J. Appl. Phys.* **102**, 083707 (2007).